

Supporting Information for

**Visible light-induced water splitting in an aqueous suspension
of a plasmonic Au/TiO₂ photocatalyst with metal co-catalysts**

Atsuhiro Tanaka^{[a]}, Kentaro Teramura^[a,b], Saburo Hosokawa^[a,b], Hiroshi
Kominami^[c], Tsunehiro Tanaka^[a,b]*

^[a] Department of Molecular Engineering, Graduate School of Engineering, Kyoto University, Kyotodaigaku Katsura, Nishikyo-ku, Kyoto 615-8510, Japan. E-mail: atsu.tana@apch.kindai.ac.jp

^[b] Elements Strategy Initiative for Catalysts & Batteries (ESICB) Kyoto University, 1-30 Goryo-Ohara, Nishikyo-ku, Kyoto 615-8245, Japan.

^[c] Department of Applied Chemistry, Faculty of Science and Engineering, Kindai University, Kowakae, Higashiosaka, Osaka 577-8502, Japan

Experimental Section

Synthesis of $\text{TiO}_2\text{-M}$ (M: Pt, Au, Pd, Rh, Ag): Loading of co-catalysts (M: Pt, Au, Pd, Rh, Ag) on TiO_2 was performed by the PD method. TiO_2 powder was suspended in 10 cm^3 of an aqueous solution of methanol (50 vol %) in a test tube, and the test tube was sealed with a rubber septum under argon (Ar). An aqueous solution of the co-catalyst source was injected into the sealed test tube and then photoirradiated for 2 h at $\lambda > 300 \text{ nm}$ by a 400 W high-pressure mercury arc (Eiko-sha, Osaka) with magnetic stirring in a water bath continuously kept at 298 K. The co-catalyst source was reduced by photogenerated electrons, and metal was deposited on the surface of the TiO_2 particles. Analysis of the liquid phase after photodeposition revealed that the co-catalyst source had been almost completely (> 99.9%) deposited on the TiO_2 particles. The resultant powder was washed repeatedly with distilled water and then dried at 310 K overnight under air.

Synthesis of $\text{TiO}_2\text{-M}$ (M: Ni, Ru): Loading of co-catalysts (M: Ni, Ru) on TiO_2 (preparation of $\text{TiO}_2\text{-M}$) was performed by the IM method. TiO_2 powder was suspended in 10 cm^3 of an aqueous solution of the co-catalyst source in a glass dish and was evaporated to dryness at 333 K. The product was dried overnight at room temperature and then calcined at 573 K for 1 h in air.

Synthesis of colloidal Au nanoparticles: Colloidal Au nanoparticles were prepared using the method reported by Frens.¹ To 750 cm^3 of an aqueous tetrachloroauric acid (HAuCl_4) solution (0.49 mmol dm^{-3}), 100 cm^3 of an aqueous solution containing sodium citrate (39 mmol dm^{-3}) was added. The solution was heated and boiled for 1 h. After the color of the solution had changed from deep blue to deep red, the solution was boiled for an additional 30 min. After the solution was cooled to room temperature, Amberlite MB-1 (ORGANO, 60 cm^3) was added to remove excess sodium citrate. After 1 h of treatment, MB-1 was removed from the solution using a glass filter.

Synthesis of Au/TiO_2 and $\text{Au}/\text{TiO}_2\text{-M}$: Loading of Au particles on the $\text{TiO}_2\text{-M}$ samples was performed by the CP method.² Preparation of $\text{TiO}_2\text{-M}$ having 1.0 wt% Au as a typical sample is described. A $\text{TiO}_2\text{-M}$ sample (168 mg) was suspended in 20 cm^3 of an aqueous solution of colloidal Au nanoparticles (0.085 mg cm^{-3}) in a test tube, and the test tube was sealed with a rubber septum under Ar. An aqueous solution of oxalic acid (50 μmol) was injected into the sealed test tube. The mixture was photoirradiated at $\lambda > 300 \text{ nm}$ by a 400 W high-pressure mercury arc under Ar with magnetic stirring in a water bath continuously kept at 298 K. The resultant powder was washed repeatedly with distilled water and then dried at 310 K overnight under air. Co-catalyst-free samples (Au/TiO_2) were also prepared by the same method using bare TiO_2 samples. When samples with different Au contents were prepared, the amount of $\text{TiO}_2\text{-M}$ (or TiO_2) was changed (volume and concentration of the Au colloidal solution being fixed). Hereafter, an Au-loaded $\text{TiO}_2\text{-M}$ sample having Y wt% of M and X wt% of Au is designated as $\text{Au}(X)/\text{TiO}_2\text{-M}(Y)$; for example, a sample having 0.5 wt% Ni and 1.0 wt% Au is shown as $\text{Au}(1.0)/\text{TiO}_2$ -

Ni(0.5).

Characterization: Diffuse reflectance spectra of the samples were obtained with a JASCO Corporation V-670 spectrometer equipped with an integrating sphere. Spectralon, which was supplied by Labsphere Inc., was used as a standard reflection sample such as BaSO₄. Morphology of the samples was observed under a JEOL JEM-2100F transmission electron microscope (TEM) operated at 200 kV in the Joint Research Center of Kindai University. X-ray photoelectron spectroscopy (XPS) measurement was conducted on an ESCA-3400 spectrometer (Shimadzu, Japan). A sample was mounted on a silver sample holder by using conductive carbon tape and analyzed using Mg K α radiation in a vacuum chamber in 0.1-eV steps. The position of the carbon peak (284.6 eV) for C1s was used to calibrate the binding energy for all the samples. Ni K-edge (8.3 keV) X-ray absorption fine structure (XAFS) measurements were made in the fluorescence mode at the BL01B1 beamline of the SPring-8 synchrotron radiation facility (Hyogo, Japan). A typical data reduction procedure (e.g., background removal or normalization) was carried out with Athena (version 0.9.20).

Photocatalytic reaction: Reactions were conducted in a Pyrex side-irradiation vessel connected to a glass closed gas circulation system. A 300-mg sample of Au/TiO₂-M powder was dispersed in pure water (300 cm³) using a magnetic stirrer, and this reactant solution was evacuated under vacuum several times to completely remove any residual air, following which a small amount of Ar gas was introduced into the reaction system prior to irradiation under a 300 W xenon lamp (Cermax, PE300BF) filtered with a various filters with a 15 A output current. The amounts of H₂ and O₂ in the gas phase were measured using a Shimadzu GC-8A gas chromatograph equipped with an MS-5A column.

References

- 1) Frens, G. *Nat. Phys. Sci.* **1973**, *241*, 20-22.
- 2) Tanaka, A.; Ogino, A.; Iwaki, M.; Hashimoto, K.; Ohnuma, A.; Amano, F.; Ohtani, B.; Kominami, H. *Langmuir* **2012**, *28*, 13105-13111.

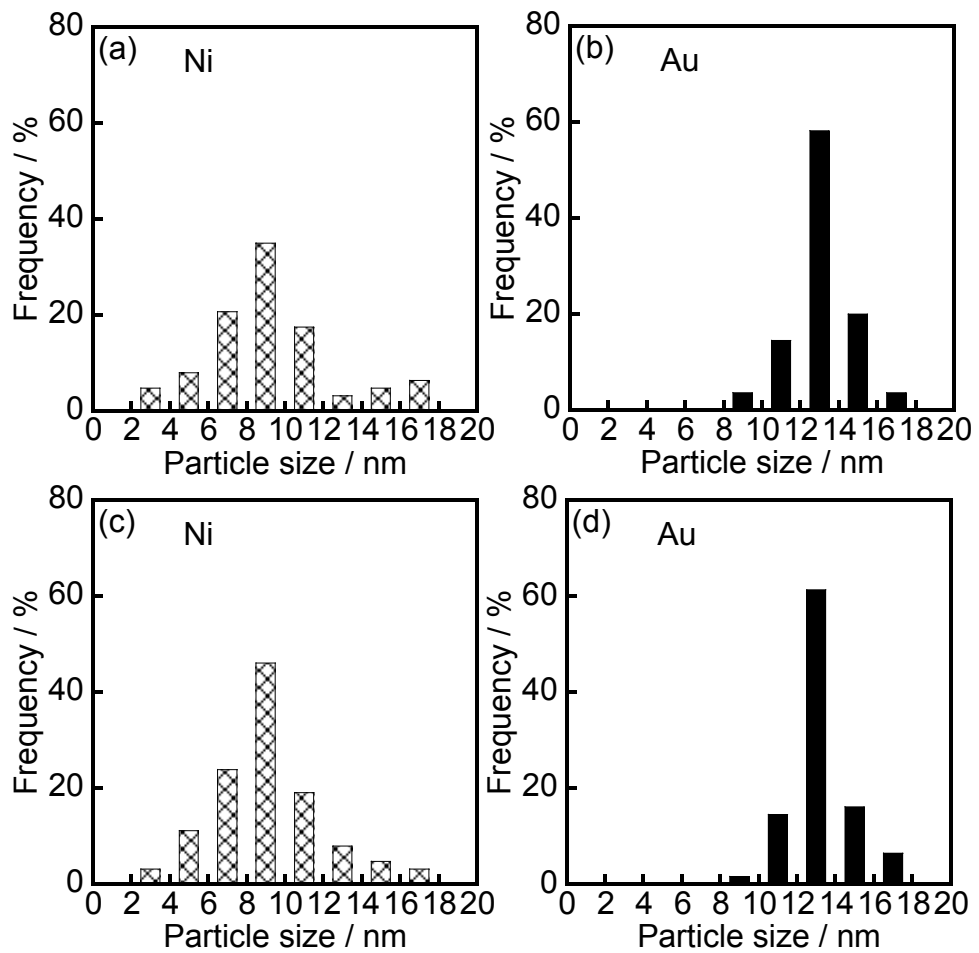


Figure S1 Particle size distributions of (a) $\text{TiO}_2\text{-NiO}_x(0.5)$, (b) $\text{Au}(1.0)/\text{TiO}_2$ and (c and d) $\text{Au}(1.0)/\text{TiO}_2\text{-NiO}_x(0.5)$.

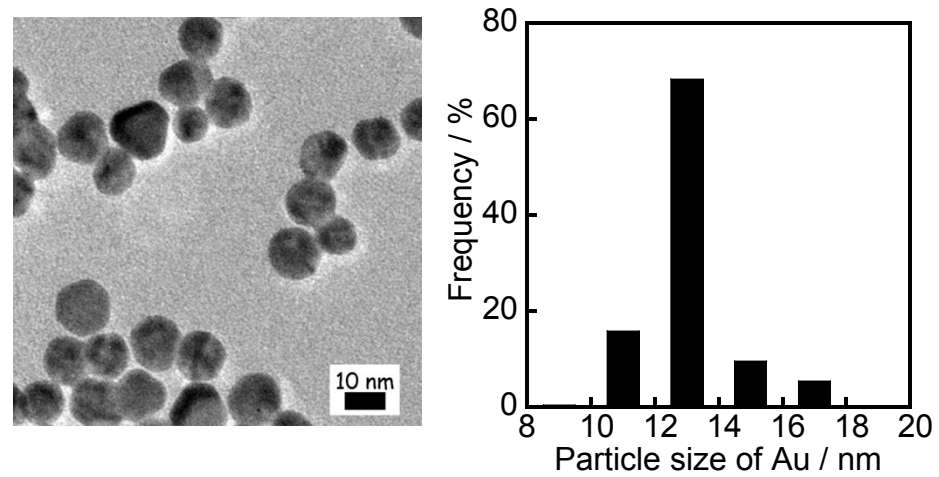


Figure S2 TEM photograph (left) and of particle size distribution (right) of Au colloid.

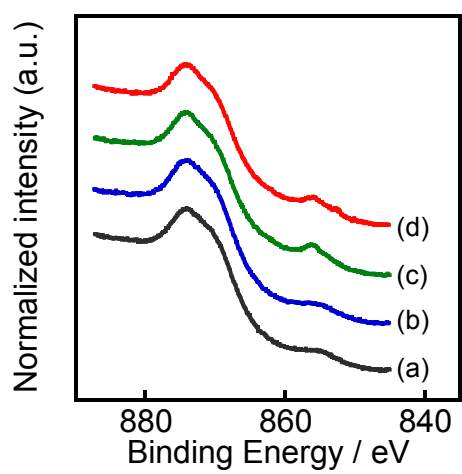


Figure S3 Normalized XPS spectra of (a) TiO_2 , (b) $\text{Au}(1.0)/\text{TiO}_2$, (c) $\text{TiO}_2\text{-NiO}_x(0.5)$ and (d) $\text{Au}(1.0)/\text{TiO}_2\text{-NiO}_x(0.5)$.

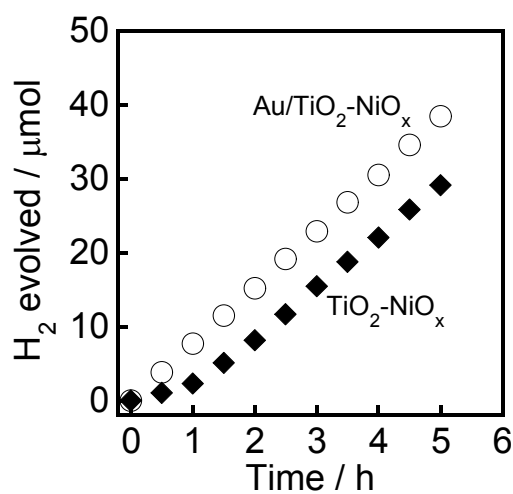


Figure S4 Time courses of evolution of H_2 from methanol over $\text{TiO}_2\text{-NiO}_x(0.5)$ and $\text{Au}(1.0)/\text{TiO}_2\text{-NiO}_x(0.5)$ under irradiation of UV light from a Xe lamp.

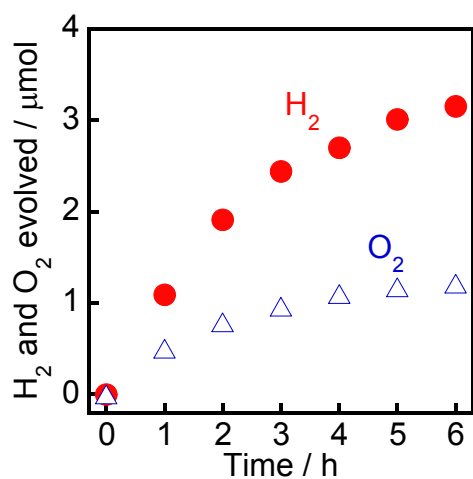


Figure S5 Time courses of evolution of H_2 and O_2 from water over $\text{Au}(1.0)/\text{TiO}_2\text{-Pt}(0.5)$ under irradiation of visible light from a Xe lamp with L42 filter.

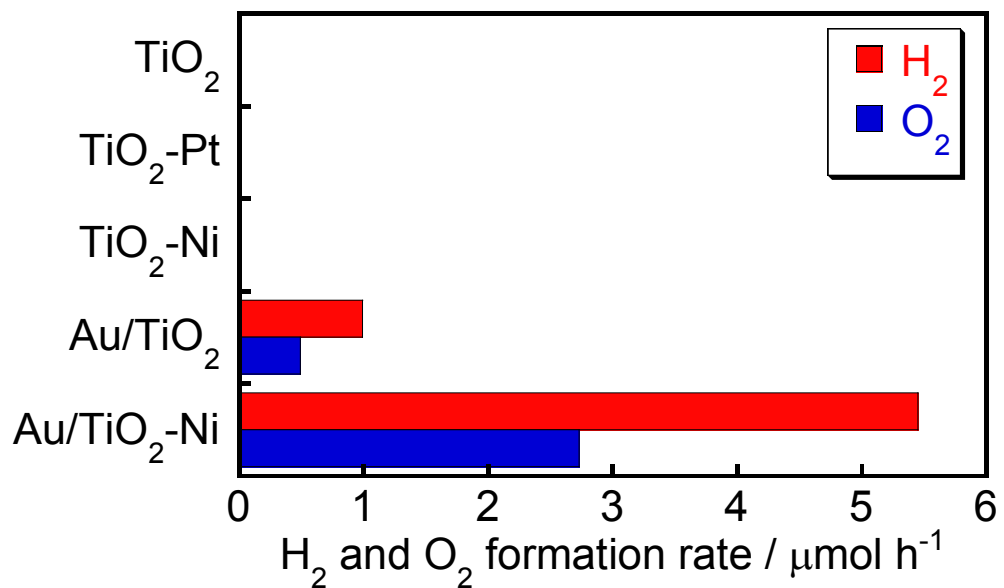


Figure S6 Rates of formation of H_2 and O_2 from water over various photocatalysts under irradiation of visible light from a Xe lamp with an L-42 cut-filter.

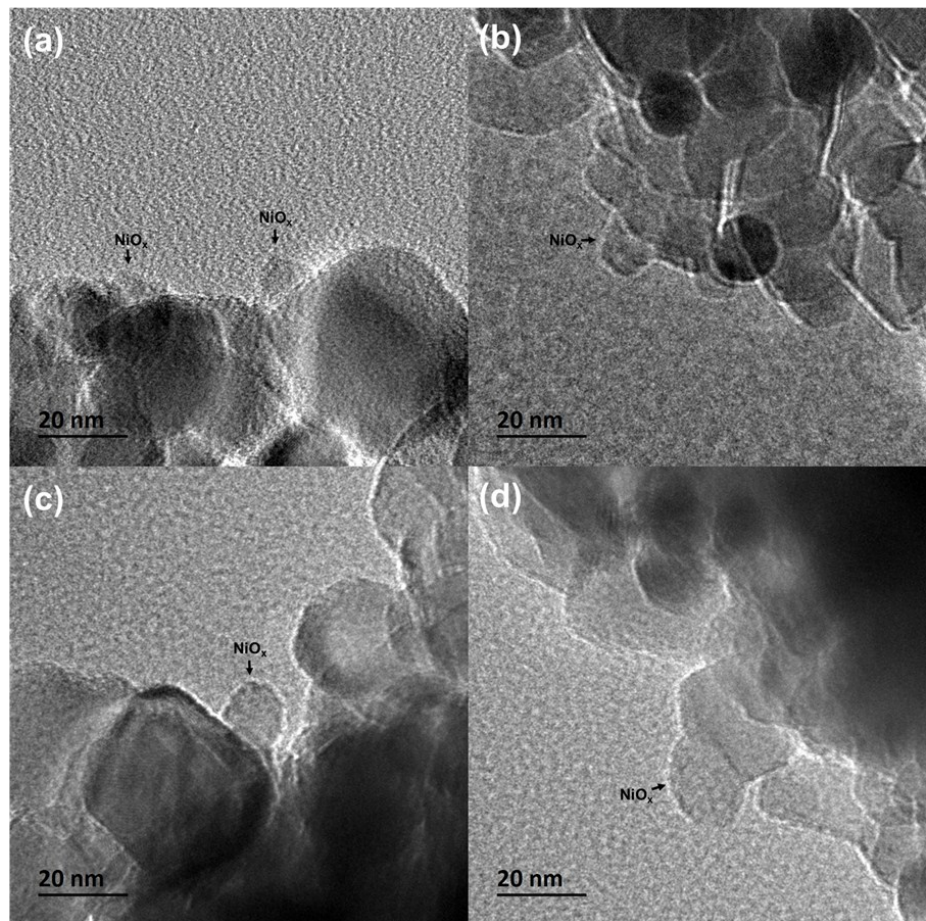


Figure S7 TEM photographs of (a) Au(1.0)/TiO₂-NiO_x(0.1), (b) Au(1.0)/TiO₂-NiO_x(0.5), (c) Au(1.0)/TiO₂-NiO_x(1.0), and (d) Au(1.0)/TiO₂-NiO_x(2.0).

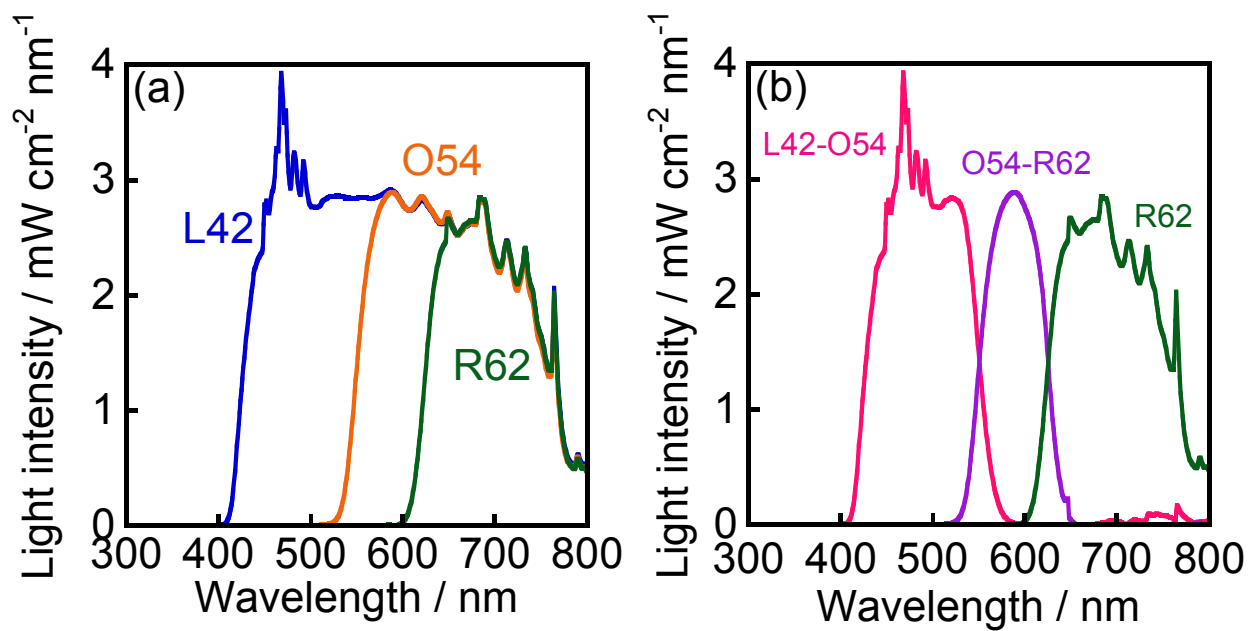


Figure S8 (a) Spectra of visible light from Xe lamp with L42, O54 and R62 cut filter; (b) subtraction spectra (L42-O54 and O54-R62), and spectrum with R62 same for (a).

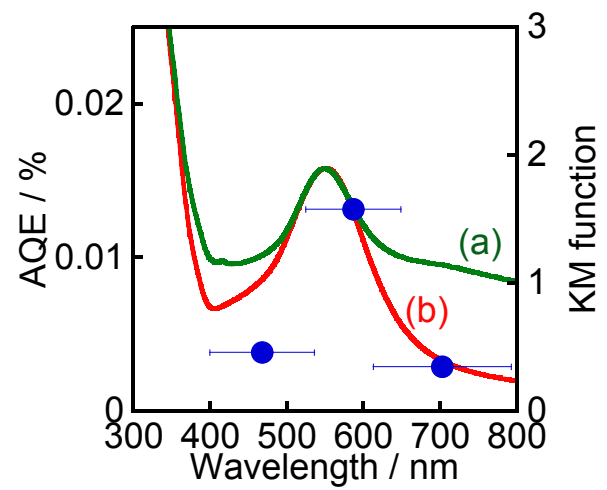


Figure S9 Absorption spectrum of (a) $\text{Au/TiO}_2\text{-NiO}_x$ and (b) Au/TiO_2 measured with barium sulfate as a reference (right axis) and action spectra (circles) in water splitting (left axis).

We analyzed the effect of wavelength of light and added an action spectrum as Figure S9. Data used for calculation of AQE were added in Table S1.

Table S1 Data used for calculation of AQE

	L42-O54	O54-R62	R62
H ₂ formation rate /μmol h ⁻¹	1.1	2.8	1.2
Photon flux /μmol h ⁻¹	57406	42582	82950

It should be noted that photon flux was smallest at [O54-R62] but H₂ formation rate was largest. On the other hand, H₂ formation rates at [L42-O54] and R62 were smaller than that at [O54-R62] in spite of larger values of photon flux. These results mean that, in Figure S9, we observe compressed tendency of AQE against wavelength of light.